



Cite this: *Nanoscale Adv.*, 2021, **3**, 2017

## Investigating the remediation potential of iron oxide nanoparticles in Cu-polluted soil–plant systems: coupled geochemical, geophysical and biological approaches<sup>†</sup>

E. Demangeat, <sup>a</sup> M. Pédro, <sup>a</sup> A. Dia, <sup>a</sup> M. Bouhnik-Le-Coz, <sup>a</sup> P. Roperch, <sup>a</sup> G. Compaoré<sup>a</sup> and F. Cabello-Hurtado<sup>\*b</sup>

Although the use of iron oxide nanoparticles (IONPs) has high potential in remediation and agriculture, a major hindrance to their use includes the risk of contamination of soil and water resources with underexplored effects of IONPs on biota. The fate, phytotoxicity and remediation potential of IONPs are investigated with soil column experiments using 7 nm-sized magnetite ( $Fe_3O_4$ ) nanoparticles (magnNPs) and sunflower (*Helianthus annuus*). Control soil, magnNP-containing soil (10 g magnNPs per kg soil), copper-polluted soil (500 mg Cu per kg soil) and copper-polluted soil containing magnNPs (10 g magnNPs per kg soil and 500 mg Cu per kg soil) support sunflower growth for 57 and 95 days. In magnNP-exposed plants, the occurrence of magnNPs does not affect the growth of the vegetative aerial parts and photosynthetic efficiency. Decreased lipid peroxidation indicates an enhanced antioxidant enzymatic response of magnNP-exposed plants. In plants grown in Cu- and magnNP–Cu-soils, the physiological and biochemical impacts of excess copper are clearly identified, resulting in growth retardation, decreased pigment contents and photosynthetic efficiency, and increased lipid peroxidation and peroxidase (POD) activities. Based on magnetic susceptibility, a higher amount of magnNPs is detected after 57 days in the roots of magnNP-exposed plants ( $1400 \text{ mg kg}^{-1}$ ) than in the roots of magnNP–Cu-exposed plants ( $920 \text{ mg kg}^{-1}$ ). In the latter, magnNP internalization is likely hampered because of the plants' physiological responses to Cu toxicity. At the working Cu and magnNP concentrations, magnNPs neither decrease Cu accumulation in the plant tissues nor alleviate the overall growth retardation of sunflowers and certain phytotoxic effects induced by excess Cu. However, this study highlights several positive environmental aspects relative to magnNP use, including the harmless effects of magnNPs on sunflowers (1% magnNPs in soil) and the ability of magnNPs to influence Cu mobility in the soil (which could be even more pronounced at lower Cu concentration).

Received 6th October 2020  
Accepted 30th January 2021

DOI: 10.1039/d0na00825g  
[rsc.li/nanoscale-advances](http://rsc.li/nanoscale-advances)

### 1. Introduction

The increasing production and use of engineered nanoparticles (NPs) has led to the significant occurrence of these new materials in the environment.<sup>1</sup> The unique properties of NPs, particularly their high reactivity (high surface-to-volume ratio), have fuelled their employment in the technological, medical, agricultural and environmental fields.<sup>2–7</sup> As a result, their direct intentional (agrochemical spraying) or unintentional deposition (aerial deposition, urban waste) in the environment has provided multiple ways for NPs to enter ecosystems, through

the air, soil or water.<sup>8</sup> Amongst these NPs, iron oxide nanoparticles (IONPs) may originate from their use in the environmental sector, especially for soil and water decontamination, where IONPs show promising potential for metal and metalloid removal.<sup>9,10</sup> As a consequence, considerable research is needed to assess the impacts and fate of IONPs in the environment and the interactions that ensue from the presence of IONPs in natural media. Considering the key role played by plants within ecosystems, special attention has been paid to elucidate the effects of IONPs on plants.<sup>11–13</sup>

One of the first challenges to deciphering the physiological and biochemical responses of plants to IONP exposure is to understand the complex interplay in between IONP properties, biota and soil. Abiotic (pH, salinity, ionic strength, temperature, light, etc.) and biotic conditions (related to plant roots or rhizosphere microfauna and microbial, bacterial and fungal activities)<sup>8,14–16</sup> are important and need to be considered as they

<sup>a</sup>Univ Rennes, CNRS, Géosciences Rennes, UMR 6118, 35000 Rennes, France. E-mail: [ed.demangeat@gmail.com](mailto:ed.demangeat@gmail.com)

<sup>b</sup>Univ Rennes, CNRS, ECOBIO, UMR 6553, 35000 Rennes, France. E-mail: [francisco.cabello@univ-rennes1.fr](mailto:francisco.cabello@univ-rennes1.fr)

† Electronic supplementary information (ESI) available. See DOI: [10.1039/d0na00825g](https://doi.org/10.1039/d0na00825g)

can influence IONP persistence in a medium, as well as IONP mobility, bioavailability, uptake and toxicity in plants.<sup>17</sup> Previous studies showed that the uptake of IONPs by plants is directly related to the individual IONP size, surface charge, and surface coating.<sup>14</sup> Besides, IONP concentration in the medium as well as the physico-chemical properties and composition of the medium, the plant species, the plant growth stage and the plant exposure route all together play a critical role in driving IONP uptake and IONP effects on the plants exposed.<sup>18-20</sup>

Because of these multiple interfering parameters, the effects of IONPs on plants are variable and often appear quite hazardous, ranging from positive to lethal.<sup>21,22</sup> The adverse effects of IONPs on plants generally result from oxidative stress and/or from decreased cellular exchange with the media due to particle binding onto the cell surface.<sup>23</sup> Once in the cell, metal nanoparticles could interfere with the electron transport chain of both chloroplasts and mitochondria, which may result in an oxidative burst, as observed by increased reactive oxygen species (ROS) concentration.<sup>24</sup> Although ROS can act as secondary messengers in the stress signal transduction pathway, excessive ROS production can cause oxidative stress, which damages plants by oxidizing photosynthetic pigments, membrane lipids, proteins and nucleic acids.<sup>25,26</sup> On the other hand, IONPs can indirectly impact plant metabolism. In particular, IONPs can react with pollutants in soils and soil solutions, such as heavy metals or pesticides and other contaminants, and thus modify their availability, transport and toxicity.

Along with the use of pesticides, fungicides, industrial effluents and wastewater irrigation, copper (Cu) is commonly found in agricultural soils where high Cu concentrations have raised great concern for sustainable agricultural production.<sup>27</sup> For example, the use of the Bordeaux mixture has seriously increased Cu pollution in European vineyard soils (200–500 mg Cu per kg soil)<sup>28</sup> compared to uncontaminated soils (3 to 100 mg Cu per kg soil).<sup>29</sup> Although Cu is an essential micronutrient present in many plant proteins, excess Cu in soil results in phytotoxicity, including leaf chlorosis and stunted plant growth (particularly root growth). Copper phytotoxicity also leads to a reduced uptake and accumulation of other mineral nutrients, thus disturbing important plant biochemical processes.<sup>30,31</sup> Copper was notably found to prevent Fe absorption, highlighting an antagonistic relationship between Cu and Fe uptake.<sup>31</sup> In addition, different studies have described Cu affinity and adsorption onto IONPs<sup>32,33</sup> suggesting that the presence of IONPs could affect the expected Cu phytotoxicity in polluted soil. On the other hand, Cu bioavailability depends upon soil physico-chemical parameters and CEC (cation exchange capacity) and the total soil Cu content.<sup>34</sup> Thus, much of the Cu present in soils is not easily available to plants because of the tight binding of Cu<sup>2+</sup> to soil organic matter and other colloids.<sup>35</sup>

Studies devoted to the interactions between plants and IONPs are at the heart of multiple research investigations, with important implications for agricultural practices. To exploit the potential benefits of IONPs for crops, issues concerning IONP availability, biocompatibility and behaviour in the growth culture medium need to be further investigated. In this context,

the objectives of this study were (i) to determine whether magnetite nanoparticles (magnNPs) have any toxic effects on sunflower plants at the exposed concentrations, (ii) to assess the mobility of magnNPs in soil and plants and (iii) to decipher their effects in copper-contaminated soil–plant systems. Ultimately, this study aims to shed light on the environmental risks of IONPs and their remediation potential in Cu-polluted soils, considering that these nanomaterials are already used for industrial and agricultural purposes.

## 2. Materials and methods

### 2.1. Iron oxide nanoparticle synthesis and characterization

Fe<sub>3</sub>O<sub>4</sub> nanoparticles (MagnNPs) were prepared as previously described in Demangeat *et al.* (2018)<sup>35</sup> through anaerobic (Jacomex glovebox) coprecipitation of Fe salts (FeCl<sub>2</sub>·4H<sub>2</sub>O and FeCl<sub>3</sub>·6H<sub>2</sub>O). The final black precipitate of magnNPs was washed with deoxygenated deionized water once and 5 × 10<sup>-3</sup> M NaCl solution (2 times) and then stored under anaerobic conditions.

The magnNP size was determined using high-resolution transmission electron microscopy (HR-TEM) with a JEOL100C-XII instrument (voltage 100 kV) at the THEMIS Analytical Facility at the University of Rennes 1. The magnNP samples were initially suspended in 0.005 mM NaCl (pH = 6), and the suspensions were further diluted to reach a concentration of 1 × 10<sup>-3</sup> mg L<sup>-1</sup> magnNPs before being carefully placed on 300 mesh Au grids supported with carbon film.

The magnNP surface area was measured using the multi-point N<sub>2</sub>-Brunauer Emmett Teller (BET) technique with a Coulter (SA 3100) analyser. Prior to the measurements, tubes containing 35 mL solutions (18 g L<sup>-1</sup>, 0.005 mM NaCl and pH = 6) of magnNPs were centrifuged at 4110g for 30 min. Then, the supernatant was removed, and the wet mineral pastes (concentrated at the bottom of the tubes) were placed in an oven where they were gently dried at 49 °C for 2 days. Once completely dry, the solid pieces were put in a mortar and ground with a pestle to obtain a fine powder.

To determine the pH of the zero point of charge (pH<sub>zpc</sub>), potentiometric acid–base titrations were conducted on 1 and 2 g L<sup>-1</sup> solid solutions at three ionic strengths (1 × 10<sup>-2</sup>, 5 × 10<sup>-2</sup>, and 1 × 10<sup>-1</sup> M NaCl) using a self-developed titration system with two titrators (794 Basic Titrino – Metrohm).

The Fe(II)/Fe(III) ratio of magnNPs was determined after acidic dissolution of magnNPs (12 h using 0.6 M HCl) under anaerobic conditions. Then, dissolved Fe(II) and Fe(III) concentrations were measured using the 1,10-phenanthroline colorimetric method.<sup>33</sup> At the beginning of the experiments, the Fe(II)/Fe(III) ratio was equal to 0.5. The measurement was performed on a 12 g L<sup>-1</sup> magnNP suspension in 0.005 mM NaCl, pH = 6.

### 2.2. Plant growth conditions and treatments

Plants (*Helianthus annuus* – 1 plant per column) were grown in soil columns (250 mL polypropylene measuring cylinders, VWR). The soil was held over a height of 13 cm (120 g of dry soil) maintained by a circular drilled plate (3.7 cm diameter) covered



with a nylon filter (ESI Fig. S1†). Soil solution leakage and regular sampling of leachates were allowed by an aperture created at the cylinder bottom (ESI Fig. S1†). The columns were wrapped with aluminium paper to avoid any exposure of the medium to light and algal development.

The soil used in the experiment (ESI Table S1†) was sampled in an inventoried natural observatory (the so-called Zone Atelier Armorique; <http://www.za-inee.org/en>) in the wetland area of Pleine-Fougères (Brittany, France) in the 0 to 20 cm-deep first horizon. Following its sampling, the soil was homogenized, dried and sieved through a 2.0 mm-diameter sieve. Twenty aliquots of soil (120 g each) were then constituted to obtain five replicates of the four treatments: unmodified soil (control soil), soil containing 1% magnNPs (magnNP-soil), soil polluted with Cu (Cu-soil) and soil polluted with Cu and containing 1% magnNPs (magnNP-Cu soil). Treatments involving Cu contamination were achieved by the dropwise addition of 5.5 M  $\text{CuSO}_4$  solution over a grid pattern. Because the soil initially contained Cu ( $20 \text{ mg kg}^{-1}$ ), the addition of 5.5 M  $\text{CuSO}_4$  was carried out to provide 480 mg Cu per kg soil and thereby reach  $500 \text{ mg kg}^{-1}$  in the Cu-treated soils (*versus*  $20 \text{ mg kg}^{-1}$  in control- and magnNP-soils). This concentration can be encountered in agricultural Cu-polluted soils.<sup>29,30</sup> MagnNP solution ( $12 \text{ g L}^{-1}$ ) was also dispensed drop by drop above a grid pattern in the NP-treated soils to obtain 1 wt% magnNPs and to ensure a homogeneous distribution. According to Komárek *et al.* (2013)<sup>36</sup> 1 wt% NPs provides a consistent amount of material to achieve an optimal removal of trace elements (TEs) in soil.

Because of its high biomass production and its use in phytoremediation for environmental clean-up,<sup>37,38</sup> *Helianthus annuus* was chosen for the present experiment. Prior to sowing, 60 seeds were carefully washed in a sodium hypochlorite ( $\text{NaOCl}$ ) bath (3 min) and 5 distilled water baths (12 min each). The seeds were then soaked in distilled water for 45 min under a laminar flow hood. Sunflower seed germination occurred directly in soil columns. To ensure that seedlings were obtained, 3 seeds were sown per column, and immediately after germination, only one plantlet per column was retained for growth. Cyclic growth conditions were ensured in a growth chamber, allowing 16 h light at  $22^\circ\text{C}$  and 8 h in the dark at  $18^\circ\text{C}$ , a photosynthetic photon flux density of  $160 \text{ } \mu\text{mol m}^{-2} \text{ s}^{-1}$ , and a relative humidity of 70%.

A modified Hoagland<sup>39</sup> half-strength ( $\times 0.5$ ) solution (without iron and micronutrients) or a 2 mM NaCl solution was alternately poured into the soils every 2 days at field capacity. Through this regular sprinkling, the soil was kept moist. Increased volumes of the watering solution were necessary to allow soil solution sampling every 3 to 5 days. Approximately 25 mL of soil solution was collected from each column using a peristaltic pump (set at  $1 \text{ mL min}^{-1}$ ). For each treatment (5 replicated columns), soil solutions collected from two replicates were homogenized at each sampling to allow geochemical analyses. The soil solution from the remaining replicate (for each treatment) was used for pH and Eh measurements.

At the end of the floral initiation (*i.e.*, after 57 days of growth), 4 out of 5 plants per treatment were collected for

biological analyses. Pictures were taken, and the fresh weights of the roots, aerial parts and flower buds of the plants were measured for each individual. It is noteworthy that the root weights are not provided in the results, as the whole roots could not be precisely and equally recovered from the soils (some roots were trapped in the soil or were broken). Liquid nitrogen allowed the freezing of plant samples, which were subsequently stored at  $-80^\circ\text{C}$ .

For each treatment, a fifth plant was harvested at the early fruit development stage before seed maturity (38 days after the first harvest). These plants provided samples for magnetic susceptibility measurements to study the magnNP translocation efficiency. To perform these geophysical analyses, the aerial parts of the plants were separated into 3 sections that were labelled, from the ground upwards, as follows: "AP1" (lower mid-height stem section), "AP2" (upper mid-height stem section) and "AP3" (flower head). Similarly, root (R1, R2 and R3) and soil (S1, S2 and S3) sections were labelled in the 13 cm-high soil and were numbered from 1 to 3 with increasing depth.

### 2.3. Biological assays

The following biological assays were conducted on dry plant materials. Drying was performed by lyophilization (Christ ALPHA 1-2LDplus). Drying was achieved by placing frozen plant samples into the chamber of the freeze dryer for a primary long drying (0.09 Pa for 72 h), followed by a secondary short drying stage (0.001 Pa for 24 h). Lyophilized samples were immediately sealed and preserved in a cold room. For most analyses, the vegetative lyophilized material was gently ground using an agate mortar and pestle to work on solid powders.

**2.3.1. Pigment content.** The determination of chlorophyll and carotenoid contents was achieved following a few steps. First, 5 mg dry weight (DW) of sunflower leaves was weighed and incubated at  $4^\circ\text{C}$  in 500  $\mu\text{L}$  acetone (80%). Leaf samples were soaked until complete bleaching occurred (approximately 12 h) and were then centrifuged at 12 000g. Supernatants were recovered in new tubes, and 30  $\mu\text{L}$  of each supernatant was diluted in 270  $\mu\text{L}$  of acetone (80%) in a microplate well. The chlorophyll content was determined by spectrophotometrically reading the absorbance at 470, 645 and 663 nm (spectrophotometer SAFAS FLX-Xenius – EcoChim analytical platform of Rennes 1 University). Based on the equations of Lichtenthaler and Wellburn (1983)<sup>40</sup> pigment contents were determined ( $\mu\text{g mg}^{-1}$  DW).

**2.3.2. Maximum quantum yield of photosynthesis.** Pulse-amplitude modulated (PAM) fluorescence was measured using a FluorPen FP100 on three leaves of each plant (second to fourth level of leaves from the base of the plant) after 34, 38 and 42 days of growth. The plants ( $n = 5$ ) were dark-adapted for 20 min to oxidize the PSII reaction centres. Chlorophyll *a* (Ca) fluorescence emission was then measured as described by Rohacek and Barták (1999)<sup>41</sup> and the maximum quantum yield of photosynthesis (QY) was calculated using the  $F_v/F_m$  ratio, where  $F_v$  corresponds to the difference between maximal ( $F_m$ ) and minimal fluorescence ( $F_o$ ).

**2.3.3. Determination of lipid peroxidation.** Measurement of the thiobarbituric acid reactant species (TBARS) allowed the



quantification of lipid peroxidation products. TBARS produced by the thiobarbituric acid (TBA) reaction were quantified according to the corrected TBA method as proposed by Hodges *et al.* (1999).<sup>42</sup> Briefly, 1 mL ethanol (80%) was added to 15 mg dry shoot to react for 25 min in a rotating wheel at room temperature. Samples were then centrifuged at 10 000g for 10 min, and the supernatants were collected in new tubes. Two aliquots of 200  $\mu$ L were mixed with TBA+ solution (20.0% trichloroacetic acid (p/v), 0.65% (p/v) TBA and 0.01% (w/v) butyl-hydroxytoluene) and two other aliquots with TBA-solution (20.0% trichloroacetic acid (p/v) and 0.01% (w/v) butyl-hydroxytoluene). Eventually, the samples were heated at 95 °C for 25 min, rapidly cooled to room temperature and immediately centrifuged at 10 000g for 10 min. The supernatants were recovered in new tubes, and 300  $\mu$ L were sampled and placed in a microplate. The absorbance of the supernatants was recorded at 440, 532 and 600 nm spectrophotometrically using a microplate reader (SAFAS FLX-Xenius). The results were finally expressed in terms of malondialdehyde equivalents (MDAeq) per gram of plant DW following the equations of Hodges *et al.* (1999).<sup>42</sup>

#### 2.3.4. Soluble protein extraction and quantification.

Sodium phosphate buffer (50 mM, pH 7.5) containing 1 mM Na-EDTA, 5% (w/v) PVP, 0.5% (v/v) protease inhibitor cocktail (Sigma-P9599) and 0.1% (w/v) Triton X-100 was used to prepare plant homogenates. The buffer (1.5 mL) was added to 50 mg DW of plant shoot in tubes and placed in a rotating wheel for 1 h at 4 °C. The samples were then centrifuged twice at 12 000g for 12 min, and the supernatants were collected in new tubes. Soluble protein quantification was performed spectrophotometrically based on Bradford's method (1976).<sup>43</sup> Bovine serum albumin (BSA) calibration solutions (0.1 to 1.4 mg L<sup>-1</sup>) were used to determine the protein contents. Protein extracts were kept at -80 °C until used in POD and SOD enzymatic antioxidant activity assays.

#### 2.3.5. Analysis of POD activity.

Guaiacol peroxidase (POD) activity was determined based on some modified literature.<sup>44,45</sup> The reaction mixture (300  $\mu$ L), prepared in each microplate well, contained 190  $\mu$ L deionized ultrapure water, 30  $\mu$ L potassium phosphate buffer (1 M, pH 6.5), 30  $\mu$ L guaiacol (150 mM) and 20  $\mu$ L soluble protein extract. Then, 30  $\mu$ L of H<sub>2</sub>O<sub>2</sub> (160 mM) were added to trigger the reaction, which was monitored by reading the absorbance at 470 nm ( $\epsilon_{\text{tetraguaiacol}} = 26.6 \text{ mM}^{-1} \text{ cm}^{-1}$ ) for 6 min (1 measurement every 40 seconds). The observed increase in absorbance provided the maximum rate of tetraguaiacol formation and was used to determine the enzymatic activity. The amount of enzyme that reduced 1  $\mu$ mol of H<sub>2</sub>O<sub>2</sub> per min corresponds to 1 unit (U) of POD under the assayed conditions.

#### 2.3.6. Analysis of SOD activity.

The capacity of superoxide dismutase (SOD) to inhibit the photochemical reduction of nitro blue tetrazolium (NBT) was measured following the method of Giannopolis and Ries (1977)<sup>46</sup> with few modifications. For each analysis, the following reactants were added to microplate wells: 180  $\mu$ L of deionized ultrapure water, 30  $\mu$ L of potassium phosphate buffer (500 mM, pH 7.8), 30  $\mu$ L of methionine (130 mM), 30  $\mu$ L of NBT (750  $\mu$ M) and 10  $\mu$ L of soluble protein extract. Two microplates (one exposed to light

and the other kept in the dark to correct for light-independent reactions) were necessary for the spectroscopic analyses. Before initiating the reaction, prereading was performed at 560 nm for each plate. Riboflavin (20  $\mu$ M) was then added (30  $\mu$ L) to each well to initiate the reaction, and the samples were exposed for 8 min either to light (first plate) or dark conditions (second plate). Immediately afterwards, the absorbance was read at 560 nm. Pre-read values were then subtracted from the final absorbance measurements for calculation of SOD activity, which was expressed in U mg<sup>-1</sup> protein (the unit "U" being the amount of enzyme causing 50% inhibition of the NBT reduction to blue formazan observed in the absence of the enzyme).

#### 2.4. Geochemical analyses

Major and trace element concentrations were determined by ICP-MS (Agilent 7700x) using rhenium and rhodium as internal standards. The international geostandard SLRS-5 was used to check the validity and reproducibility of the results.<sup>47</sup> Samples were prepared in a clean room in pre-washed digestion vessels (Savillex® Teflon vials) (24 h in nitric acid (1.5 M HNO<sub>3</sub>) at 45 °C, 24 h in deionized ultrapure water at 45 °C - repeated twice) and were further diluted in prewashed 50 mL tubes (24 h in nitric acid (1.5 M HNO<sub>3</sub>) at 45 °C, 24 h in deionized ultrapure water at 45 °C). For magnNPs and soil solutions, the samples were first digested for 16 h at 95 °C with subboiled nitric acid (14.6 M HNO<sub>3</sub>) and heated until complete evaporation of the solvent. The samples were eventually re-solubilized in 0.37 M HNO<sub>3</sub> with appropriate dilution(s) considering ICP-MS quantification limits. Lyophilized plant materials (shoots and roots, 50 mg) were digested in subboiled nitric acid (14.6 M HNO<sub>3</sub>) 5 times, with approximately 8 hours of evaporation on a hot plate (95 °C) between each digestion. When the samples were not completely dissolved after the first digestion, hydrogen peroxide (H<sub>2</sub>O<sub>2</sub>) was used for one or two more digestions. In addition, the presence of insoluble organic matter and minerals in root samples often meant that more digestions needed to be performed. Solids obtained after the last evaporation were solubilized in 0.37 M HNO<sub>3</sub> with appropriate dilution(s) considering ICP-MS quantification limits.

#### 2.5. Magnetic susceptibility measurements

To track and quantify magnNPs in soil and plant matrices, magnetic susceptibility measurements were performed. Magnetic susceptibility has already been employed to evidence magnetite occurrence in various environments.<sup>48</sup> In the present study, measurements were conducted with a magnetic susceptibility meter (Kappabridge AGICO KLY3). The magnetic susceptibility is the sum of three main sources. Magnetite is ferrimagnetic and has a large susceptibility range, from  $0.2 \times 10^{-3}$  to  $1.1 \times 10^{-3} \text{ m}^3 \text{ kg}^{-1}$ . In soil, clay minerals have mainly paramagnetic susceptibilities ( $\sim 15 \times 10^{-8} \text{ m}^3 \text{ kg}^{-1}$ ). Water is diamagnetic, with negative magnetic susceptibility ( $\sim -9 \times 10^{-9} \text{ m}^3 \text{ kg}^{-1}$ ), while the magnetic susceptibility of dried organic matter, which is also diamagnetic, may vary with the iron content. The magnetic susceptibility of the magnNPs was estimated at  $0.57 \times 10^{-3} \text{ m}^3 \text{ kg}^{-1}$ , within the range of expected



values for magnetite. Although the Kappabridge susceptibility meter is able to detect close to 1–2  $\mu\text{g}$  of magnetite, the low quantity of dried plant material (0.1–1 g) and uncertainties in the correction of the magnetic susceptibility of the uncontaminated matrix contributed to a detection level of magnetite estimated at 40  $\text{mg kg}^{-1}$  DW of plant material.

Before the analyses, the different plant parts and soil sections collected from the soil column experiments (95 day-old sunflowers, see Section 2.2) were first dried in an oven and stored in clean plastic containers. To account for the containers' signals and to identify any possible deviation occurring during the analyses, blanks (containers without samples) were used at the beginning and end of the acquisitions and after every three measurements. For each sample (including blanks), magnetic susceptibility measurements were repeated 10 times to ensure the validity and reproducibility of the results. Considering the actual weight of the material, mass susceptibilities ( $\text{m}^3 \text{kg}^{-1}$ ) were then calculated. From these values, concentrations of magnNPs in the samples were determined based on the blank-corrected magnetic susceptibility of a dry sample of magnNPs (of known weight). The sample measurements were also corrected from the mainly diamagnetic signal of the magnNPs' uncontaminated matrix contributing to the final measurements (either control plants or control soils depending on the sample type).

## 2.6. Statistical analysis

Unless otherwise noted, each value was presented as the mean  $\pm$  standard error of the mean (SEM), with a minimum of three replicates. Homoscedasticity and normality were confirmed with Bartlett and Shapiro tests for each assay. Taking  $p < 0.05$  as significant, statistical analyses were conducted using the Tukey test (one-way ANOVA) to assess the significance of the means. In figures and tables, data significantly different are indicated with different letters above bars.

## 3. Results and discussion

### 3.1. Nanoparticle characterization

MagnNP properties were studied prior to their introduction into the soils. According to HR-TEM analyses (ESI Fig. S2†),

magnNPs have well crystallized rounded shapes with a mean diameter of 7 nm. From BET measurements, the specific surface area of the magnNPs was  $\sim 115 \text{ m}^2 \text{ g}^{-1}$ . From the potentiometric titration measurements, the magnNPs'  $\text{pH}_{\text{zpc}}$  was determined at 6.2. Using the phenanthroline method, the initial  $\text{Fe(II)}/\text{Fe(III)}$  ratio of magnNPs was determined to be 0.45 under anaerobic conditions which dropped to 0.3 after the addition of the suspension to the soil samples under aerobic conditions.

### 3.2. Physiological and biochemical responses of plants exposed to magnNPs in the context of Cu pollution

**3.2.1. Growth parameters.** The fresh weights of the aerial parts of 57 day-old plants exposed to magnNPs ( $8.8 \pm 0.8 \text{ g}$ ) were not significantly different from those of control plants ( $9.1 \pm 0.7 \text{ g}$ ), except for flower buds. Although flowering was not impacted by the magnNPs, three out of four flower buds exhibited growth retardation, resulting in a significant decrease (by 53%) in the mean fresh weight of the flowers after 57 days of growth (Fig. 1). Previous studies have shown that nanoparticles can impair the overall growth and development of the plants, with variable effects depending on NP properties and concentration.<sup>21</sup> In the present study, even if the occurrence of 1% magnNPs did not affect the growth of the vegetative aerial parts, the biochemical processes governing the timing of flower bud initiation may have been impacted.

For 57 day-old plants grown in Cu-polluted soils, the mean fresh weight of the vegetative aerial parts ( $4.4 \pm 0.4 \text{ g}$ ) was significantly decreased (by 55%) compared with the fresh weights of the vegetative aerial parts of the control plants (Fig. 1), and no flower buds were formed. Biomass reduction is a common feature in most plant species exposed to excess Cu.<sup>31,49</sup> In fact, Cu toxicity has been reported to reduce the biomass of different plant species, thereby contributing to the retardation of normal growth.<sup>50</sup> For sunflower plants grown in magnNP–Cu soils, the mean fresh weight of the vegetative aerial parts ( $3.6 \pm 0.4 \text{ g}$ ) was also significantly decreased (by 58%) compared with the mean fresh weight of the vegetative aerial parts of the control plants (Fig. 1). This decrease was not significant compared with the mean fresh weights of the vegetative aerial parts of Cu-plants. In addition, although the fresh

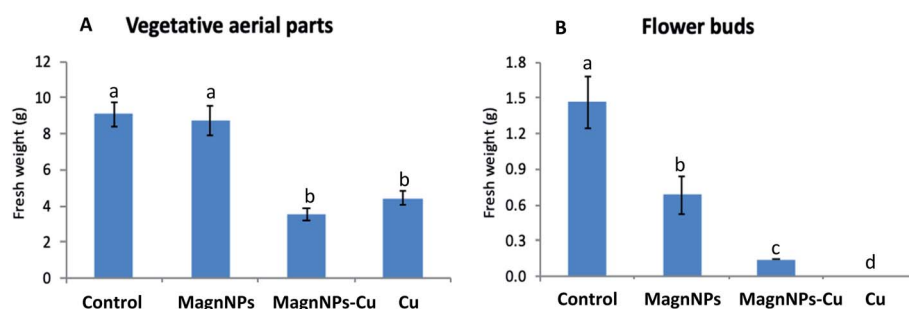


Fig. 1 Fresh weights (g) of (A) the vegetative aerial parts (stems and leaves) and (B) the flower buds (right graph) of the plants measured after 57 days of growth in the four soils (control soil, soil with 1 wt% magnNPs, soil with copper ( $500 \text{ mg kg}^{-1}$ ) and soil with both copper and magnNPs). Data represent the mean  $\pm$  SEM ( $n = 4$ ) of the fresh weights of the plants. Different letters above bars indicate significant differences ( $p < 0.05$ ). The fresh weights of the flower buds of Cu plants are not presented (right graph) and could be approximated to zero since no flower buds developed on these plants (no samples).



weights of the roots were not readily quantifiable here (roots were not well separated from the soil and wholly recovered), visual observations provided a sufficient basis to note that root growth was highly impacted by Cu pollution. The inhibitory action of excess Cu on the vegetative growth (aerial parts and roots) of plants likely stemmed from the biochemical impacts induced by Cu, which can also result in reduction in cell division, and toxic effects on photosynthesis, respiration and protein synthesis.<sup>51</sup> Although the development of flower buds was severely affected (decrease by 92% of the mean fresh weight), it was not completely inhibited in plants grown in magnNP–Cu soils. Hence, the occurrence of magnNPs could somehow protect flower buds from excess Cu in soils, as suggested by the initiation of flower buds in the 57 day-old magnNP–Cu treated plants.

**3.2.2. Pigment contents and photosynthetic efficiency.** The highest contents of chlorophylls ( $Ca$  and  $Cb$ ) and carotenoids ( $K$ , which includes xanthophylls and carotenes) were measured in the leaves of the control plants ( $Ca = 2.6 \mu\text{g mg}^{-1}$  DW;  $Cb = 0.82 \mu\text{g mg}^{-1}$  DW and  $K = 0.61 \mu\text{g mg}^{-1}$  DW) (Fig. 2). In the leaves of the plants exposed to the three other treatments (magnNPs, magnNPs–Cu and Cu), the pigment contents were decreased. The treatment with magnNPs alone decreased the  $Cb$  content by  $\sim 15\%$  and the carotenoid content by  $\sim 26\%$  (Fig. 2). In plants grown in magnNP–Cu-soils,  $Ca$  and  $Cb$  were decreased by 31 and 36%, respectively, and  $K$  was decreased by

41%, and in Cu-soils,  $Ca$  and  $Cb$  were decreased by 27 and 32%, respectively, and  $K$  was decreased by 43% (Fig. 2). No significant differences for  $Ca$ ,  $Cb$  and  $K$  were calculated between magnNP–Cu and Cu treatments, meaning that magnNPs neither alleviated nor exacerbated the effects induced by excess Cu on the pigment contents. Chlorophyll *a* and *b* are light collectors, while carotenoids have multiple functions in light capture, photoreception and several other processes.<sup>51</sup> Regardless of the stress origin, changes in photosynthetic pigment compositions can affect plant functioning at different organizational levels.<sup>52</sup> However, according to the present results, none of the treatments affected the  $Ca/Cb$  ratio (Fig. 2).

Several studies further showed that IONPs, as well as other NPs (CuO, Ag), can affect the pigment concentrations and the photosynthetic activity of the exposed plants.<sup>21,23,53</sup> In the present study, however, no further biological impacts resulting from sunflower exposure to magnNPs alone were directly associated with compositional changes in pigment contents. In particular, the maximum quantum yield of photosynthesis (QY) of 42 day-old plants exposed to magnNPs (QY =  $0.831 \pm 0.003$ ) was not significantly modified as compared to that of control plants (QY =  $0.836 \pm 0.002$ ) (Table 1). However, Cu toxicity affected the maximum quantum yield of photosynthesis, which was decreased to a greater extent in Cu plants (QY =  $0.770 \pm 0.004$ ) than in magnNP–Cu plants (QY =  $0.816 \pm 0.004$ ) after 42 days (Table 1). This observation suggests that magnNPs reduced

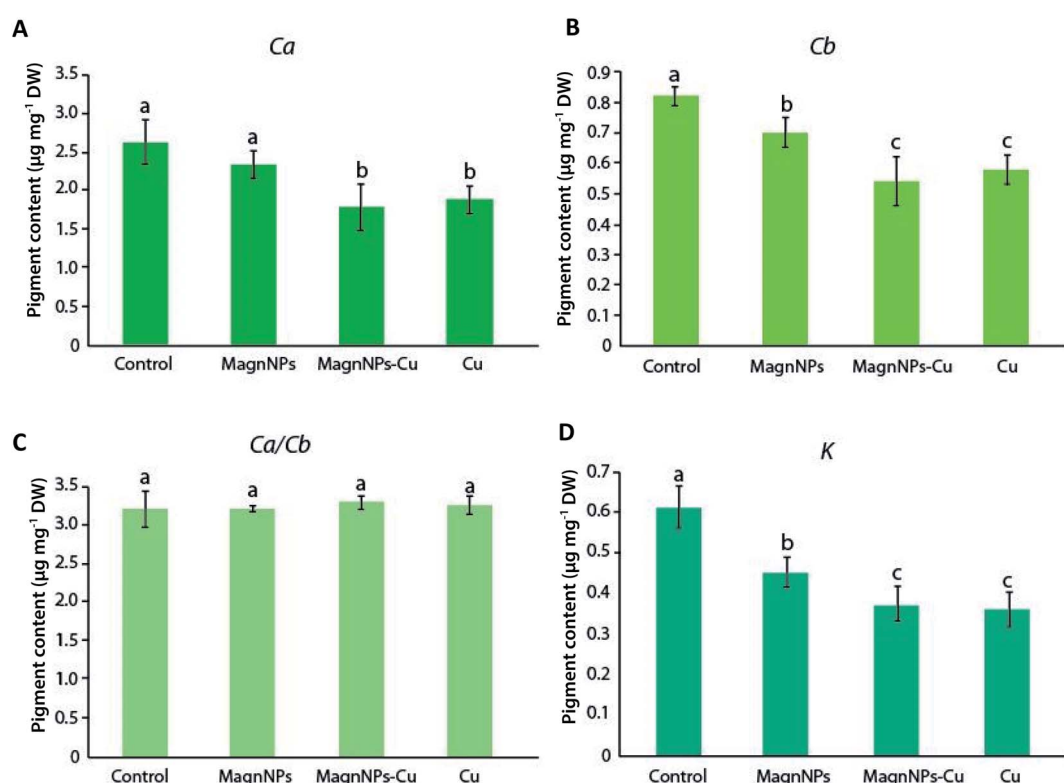


**Fig. 2** Pigment contents ( $\mu\text{g mg}^{-1}$  DW) measured in the leaves of sunflowers: (A)  $Ca$  = chlorophyll *a*; (B)  $Cb$  = chlorophyll *b*; (C)  $Ca/Cb$  = chlorophyll *a/b* ratio; (D)  $K$  = carotenoids (xanthophylls + carotenes). Data represent the mean  $\pm$  SEM ( $n = 4$ ) of the pigment contents measured in the leaves of sunflowers grown for 57 days in the four studied soils (control soil, soil with 1 wt% magnNPs, soil with copper (500 mg per kg soil) and soil with both copper and magnNPs). Different letters above the bars indicate significant differences ( $p < 0.05$ ).



**Table 1** Quantum yield (QY) measured on the leaves of 34, 38 and 42 day-old sunflowers (control, magnNP, magnNP–Cu and Cu columns). Data represent the mean  $\pm$  SEM ( $n = 5$ ). Different letters indicate significant differences between treatments in peer groups (in terms of age) ( $p < 0.01$ )

	Control	MagnNPs	MagnNPs–Cu	Cu
34 day-old	$0.829 \pm 0.002^A$	$0.823 \pm 0.001^A$	$0.811 \pm 0.006^B$	$0.757 \pm 0.005^C$
38 day-old	$0.833 \pm 0.001^A$	$0.824 \pm 0.002^A$	$0.812 \pm 0.006^B$	$0.762 \pm 0.004^C$
42 day-old	$0.836 \pm 0.002^A$	$0.831 \pm 0.003^A$	$0.816 \pm 0.004^B$	$0.770 \pm 0.004^C$

Cu phytotoxicity with regard to chloroplast functioning. Lower chlorophyll content, and inactivation of enzymes and other proteins (relating to the photosynthesis process and to the alteration of thylakoid membranes) were reported resulting from Cu toxicity.<sup>54,55</sup> In plant chloroplasts, Cu is associated with plastocyanin protein, an essential component of the photosynthetic electron transport chain between cytochrome b<sub>6</sub>f and photosystem I (PSI).<sup>56</sup> Thus, Cu deficiency can reduce PSI electron transport due to a decreased formation of plastocyanin.<sup>56</sup> On the other hand, excess Cu has been demonstrated to strongly affect the chloroplast structure with degradation of grana stacks and stroma lamellae.<sup>28,31,56</sup> Furthermore, excess Cu usually induces chlorosis and necrosis of leaves, resulting from the inhibition of pigment accumulation and the decrease in chlorophyll integration into photosystems.<sup>27,54</sup>

**3.2.3. Oxidative stress and antioxidant response.** After oxidative stress, unstable and reactive lipid peroxides – decomposing into different TBARS such as malondialdehyde (MDA) – originate from lipid peroxidation in cells.<sup>57</sup> In the present study, the TBARS measurements were the lowest in plants exposed to magnNPs ( $139.9 \pm 10.0$  MDAeq nmol g<sup>-1</sup> DW) (Fig. 3). As the TBARS content reflects the degree of oxidative injury to a plant cell, the decreased TBARS content is inferred to result from the protective effect of plants against lipid peroxidation.<sup>56</sup> Thus, magnNPs likely induced a protection against lipid peroxidation, which was not observed in the other treatments. The protective effect of IONPs against lipid peroxidation was recently highlighted for different plant species<sup>58–60</sup> triggering the protective antioxidant system against ROS. Oxidative stress is generally due to enhanced accumulation of ROS, particularly O<sub>2</sub><sup>•-</sup> and H<sub>2</sub>O<sub>2</sub> in chloroplasts, mitochondria, and

peroxisomes.<sup>61</sup> In fact, the balance between ROS production and the activities of antioxidative enzymes determines whether oxidative signalling and/or damage will occur.<sup>25</sup> In the present study, the decreased TBARS content in magnNP-plants was correlated with increased antioxidant POD activity ( $45.7 \pm 3.8$  U mg<sup>-1</sup> protein), which was enhanced relative to that measured in control plants ( $28.3 \pm 1.8$  U mg<sup>-1</sup> protein) (Fig. 3). It has been demonstrated that increased SOD and POD activities provide better plant protection mechanisms against oxidative damage.<sup>61–63</sup> In particular, POD, by catalysing the reaction between H<sub>2</sub>O<sub>2</sub> and ROOH to H<sub>2</sub>O and R-OH, directly fights against cell damage.<sup>64,65</sup> Thus, the decrease in the TBARS content along with the increase in POD activity likely suggests that the antioxidant response acted effectively against ROS (avoiding ROS overproduction and the induced oxidative damage).

The TBARS content increased from  $208 \pm 5$  MDAeq nmol g<sup>-1</sup> DW in plants grown in control soils to  $229.4 \pm 7.5$  MDAeq nmol g<sup>-1</sup> DW in Cu-exposed plants. In response to Cu pollution, plant cells likely accumulate ROS, which cause lipid peroxidation of membranes and possibly induce some further metabolic disorders, leading to oxidative stress.<sup>29,31</sup> As indicated by increased TBARS content, ROS overproduction was not compensated by SOD and POD enzymatic activities (Fig. 3). In the presence of transition metals such as Fe<sup>2+</sup> and Cu<sup>2+</sup>, H<sub>2</sub>O<sub>2</sub> can break down into damaging OH<sup>•</sup> in the successive Haber–Weiss and Fenton reactions.<sup>66</sup> In plants exposed to excess Cu, the conversion of H<sub>2</sub>O<sub>2</sub> into OH leads to lipid peroxidation, perturbation of the mitochondrial and photosynthetic electron transport chains, and substantial damage to DNA and protein expression.<sup>67</sup> Despite the excess Cu in the soil, a decreased lipid

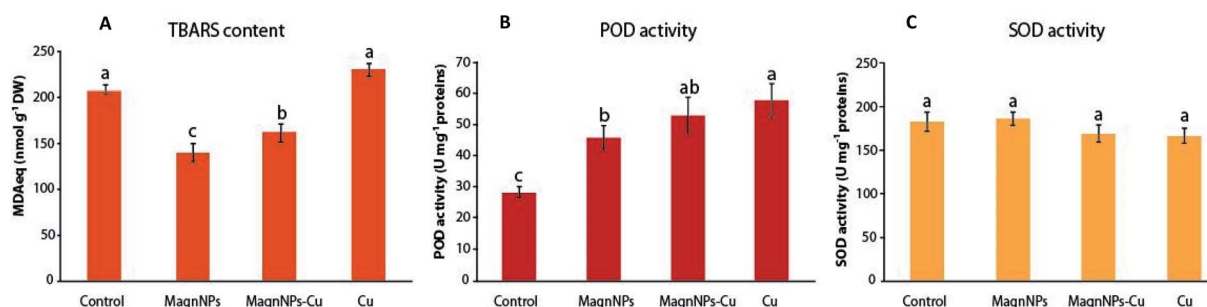


**Fig. 3** Lipid peroxidation and antioxidant activities measured in the leaves of sunflowers grown for 57 days in the four studied soils (control soil, soil with 1 wt% magnNPs, soil with copper ( $500 \text{ mg kg}^{-1}$ ) and soil with both copper ( $500 \text{ mg kg}^{-1}$ ) and magnNPs (1 wt%)): (A) TBARS content (nmol MDAeq per g DW), (B) POD activity (U mg<sup>-1</sup> protein) and (C) SOD activity (U mg<sup>-1</sup> protein). Data represent the mean  $\pm$  SEM ( $n = 4$ ). Different letters above the bars indicate significant differences ( $p < 0.05$ ).



peroxidation ( $161.3 \pm 9.9$  MDAeq nmol g<sup>-1</sup> DW) was observed in plants exposed to magnNPs–Cu compared to Cu-exposed plants. Along with the decreased TBARS content, POD was increased ( $52.7 \pm 5.9$  U mg<sup>-1</sup> protein) – close to that measured in Cu-polluted plants ( $57.5 \pm 5.2$  U mg<sup>-1</sup> protein) – and it is possible that magnNPs also influenced the activity of other antioxidant enzymes and systems.

### 3.3. Fate of magnNPs in soil-plant systems: implications for Cu-polluted soils and plants

#### 3.3.1. Uptake and translocation of magnNPs from soil to plant

*Uptake of magnNPs by the roots.* Based on magnetic susceptibility measurements, magnNPs were detected in the tissues (particularly in the roots) of magnNP- and magnNP–Cu-treated plants, with increasing concentrations over time (Tables 2 and 3, and ESI Tables S2 and S3†). When IONPs reach the soil–root interface, the first step of uptake consists of the adsorption of IONPs onto the root surface, as suggested by SEM-EDS analyses (ESI Fig. S3†). This adsorption is strongly based on the IONP surface charge<sup>14</sup> and generally, root surfaces are negatively charged, meaning that positively charged NPs are more likely to adsorb and accumulate on the root surface. Then, at the root cellular level, magnNPs are expected to interact with the plant cell wall before penetration into the cell and subsequent intracellular transportation.<sup>68</sup> Indeed, the entry of aggregated magnNPs is restricted to the pore size of the cell walls, which ranges between 5 and 20 nm in diameter<sup>12,69</sup> although new pores or wounds can form due to NP deposition.<sup>12,57</sup> In fact, several uptake mechanisms are still under consideration to explain NP translocation, such as the symplastic, apoplastic and endocytic pathways, which are considered significant alternatives to allow the passage of magnNPs through plant physiological barriers.<sup>14,21,70</sup>

According to the measurements of magnetic susceptibility (Tables 2 and 3), the amount of magnNPs was higher in the roots of magnNP-treated plants than in those of magnNP–Cu plants, highlighting that Cu likely affected the uptake process in root tissues. Direct physiological and biochemical impacts of Cu on plants may be responsible for the observed decreased magnNP uptake. As noted earlier (Section 3.1.1), the root biomass was severely decreased in sunflowers exposed to Cu- and magnNP–Cu-soils. Previous studies showed that under excess Cu, the primary root growth is indeed decreased, along

**Table 2** Concentrations of magnNPs (mg kg<sup>-1</sup>) in the sunflower tissues (stems, leaves, flowers and roots) calculated from magnetic susceptibility measurements (ESI Table S2). Sunflower plants were harvested and exposed to 1 wt% magnNPs and/or Cu (500 mg kg<sup>-1</sup>) in soil columns for 57 days. Data represent the mean  $\pm$  SEM ( $n = 4$ ). Different letters indicate significant differences between treatments and among plant parts ( $p < 0.05$ ). The quantification limit (QL) was determined at QL = 40 mg kg<sup>-1</sup>

	Roots	Stem	Leaves	Flowers
MagnNPs	$1400 \pm 310^{\text{A}}$	<QL	<QL	<QL
MagnNPs–Cu	$920 \pm 560^{\text{A}}$	<QL	<QL	<QL

**Table 3** Concentrations of magnNPs (mg kg<sup>-1</sup>) in the sunflower roots and aerial parts (stems, leaves), and in the soil samples (initially 1 wt% magnNPs) calculated from magnetic susceptibility measurements (ESI Table S3). Sunflower plants were harvested after 95 days of exposure to 1% magnNPs and/or Cu (500 mg kg<sup>-1</sup>) in soil columns. In each column, three sections were made with regard to the height of the aerial parts (increasing height from AP1 to AP3) and depth (increasing depth from 1 to 3) for roots (R) and soils (S). Data represent the mean  $\pm$  SEM, and different letters indicate significant differences between treatments and among plant parts ( $p < 0.05$ ). The quantification limit (QL) was determined at QL = 40 mg kg<sup>-1</sup>

		MagnNPs	MagnNPs–Cu
Aerial parts	AP3	<QL	<QL
	AP2	<QL	<QL
	AP1	$40 \pm 10^{\text{A}}$	<QL
Roots	R1	$2260 \pm 670^{\text{B}}$	$1610 \pm 500^{\text{BC}}$
	R2	$2810 \pm 510^{\text{B}}$	$1090 \pm 490^{\text{C}}$
	R3	$2520 \pm 560^{\text{B}}$	$660 \pm 431^{\text{C}}$
Soil	S1	$10\ 060 \pm 200^{\text{D}}$	$11\ 500 \pm 500^{\text{E}}$
	S2	$9360 \pm 320^{\text{D}}$	$10\ 680 \pm 410^{\text{E}}$
	S3	$9970 \pm 210^{\text{D}}$	$10\ 130 \pm 430^{\text{E}}$

with an increased density of short lateral roots.<sup>29,30,71</sup> Therefore, the access of Cu-affected plants to magnNPs in the deeper part of the column was probably reduced. Furthermore, lignin deposition has been reported in Cu-affected plant roots, leading to an impact on the uptake of nutrients and therefore possibly on that of magnNPs in plant roots.<sup>71</sup> Lastly, as previously observed in this study (Fig. 3), an increased lipid peroxidation is known to significantly affect the fluidity and permeability of the membranes and consequently the acquisition kinetics of nutrients (and thus also possibly that of magnNPs in this work).<sup>21</sup>

*Translocation of magnNPs to the aerial parts of sunflowers.* According to magnetic susceptibility measurements, magnNPs did not accumulate in the upper levels of the plant aerial parts after 57 days of growth (Table 2). However, positive signals evidenced the possible occurrence of a small amount of magnNPs in the close-to-ground section of the aerial parts after 95 days (ESI Table S3†). The amount detected (40 mg kg<sup>-1</sup>) matched the quantification limit of the method (Table 3). According to previous studies, the access of magnNPs to the aerial parts of the plants could result from a movement into the xylem vessels through the transpiration stream.<sup>72</sup> Magnetic susceptibility measurements performed in the aerial parts of magnNP–Cu plants (even in the close-to-ground parts) clearly indicated that no translocation occurred in Cu-contaminated soils. This result can be explained by the physiological impacts induced by the excess Cu on plants, such as decreased root growth – which is consistent with the lower magnNP concentrations observed in the roots of magnNP–Cu plants – and/or by a lower potential of magnNPs to translocate into the vascular system of sunflower plants.

*Mobility of magnNPs in the soils.* As observed from the magnetic susceptibility measurements performed on soil samples (Table 3), the final magnNP concentration was close to the initial introduced concentration in the soils (10 000 mg kg<sup>-1</sup>



is worth 1% of the soil dry weight). The homogeneous distribution of the magnNPs from the bottom to the top of the columns highlights that leaching had few effects on magnNP mobility. According to Table 4, the amount of Fe leached after 37 days only represents 2 mg (*i.e.*, 0.2% of the magnNPs when considering that all the measured Fe originates from the magnNPs). In fact, the aggregation of magnNPs to  $\mu\text{m}$ -sized aggregates was evidenced in a previous study<sup>35</sup> and such propensity to aggregate may result in decreased magnNP mobility in porous media.<sup>73</sup> In addition, most magnNPs were probably bound to clays and organic matter in the soil because of their high affinity for each other.<sup>73</sup> In most fine-textured soils, the strong binding of trace elements and nanoscale compounds with clays (and, to a larger extent, soil colloids displaying high specific surface area) has been shown to limit the leaching of these elements.<sup>74-76</sup>

### 3.3.2. Chemical exchanges between plants, soil and the soil solution

*Fe assimilation by sunflowers and the fate of magnNPs.* From the ICP-MS analyses, higher Fe contents were measured in magnNP ( $90.4 \pm 9.1 \text{ mg kg}^{-1}$ ) and magnNP-Cu ( $52.3 \pm 5.8 \text{ mg kg}^{-1}$ ) plant tissues compared with the Fe content measured in control ( $18.8 \pm 4.1 \text{ mg kg}^{-1}$ ) and Cu-treated plants ( $23.3 \pm 3.7 \text{ mg kg}^{-1}$ ) (Fig. 4). This observation suggests that magnNPs provided plants with a bioavailable pool of Fe or somehow enhanced Fe uptake. It also suggests that the presence of Cu limits Fe uptake and/or assimilation by plants. In fact, root exudates (organic acids, sugars, fatty acids, amino acids, and proteins) or microbial activity (*i.e.*, iron-reducing bacteria) may foster the dissolution of magnNPs and Fe release into more bioavailable forms (such as those induced by the action of phytosiderophores).<sup>77,78</sup> As observed in Table 4, the amount of Fe released in the magnNP soil solution ( $2093 \pm 655 \mu\text{g}$ ) was higher than that in the soil solutions of the control soil ( $598 \pm 78 \mu\text{g}$ ), Cu soil ( $496 \pm 16 \mu\text{g}$ ) and magnNP-Cu soil ( $549 \pm 43 \mu\text{g}$ ). In addition, more  $\text{Fe}^{2+}$  was detected in the magnNP soil solution than in the other soil solutions (Table 4), hence providing a greater source of bioavailable Fe to magnNP-exposed plants. This observation is consistent with the Eh measurements. The range of redox potentials measured in the magnNP soil solutions was higher and reached lower values (from 300 to 650 mV)

compared with those measured in the other soil solutions: control (400 to 650 mV), magnNP-Cu (450 to 600 mV) and Cu (450 to 650 mV) soil solutions. These results highlight the role of biotic reduction in driving Fe release, which was a dominant process in magnNP-soil. In Cu and magnNP-Cu soils, it is possible that excess Cu affected the soil microbial activity (*i.e.*, the microbial respiration rate, C mineralization and the ensuing pH and Eh)<sup>79</sup> thereby decreasing Fe bioreduction and leaching. In this study, the physiological impacts induced by excess Cu (Section 3.1) could also explain the decreased Fe biotic reduction observed in Cu-contaminated soil systems.

On the other hand, the total iron content measured in the aerial parts of magnNP and magnNP-Cu plants was different (Fig. 4), although similar Fe contents were initially introduced in the magnNP and magnNP-Cu systems. This observation suggests that Cu plays an important role in regulating Fe translocation from the roots to the aerial parts<sup>80</sup> both for ionic and nanoparticulate forms. The results obtained by ICP-MS for total Fe are consistent with the magnetic susceptibility measurements (Table 4). These results are also in agreement with the biochemical and physiological impacts induced by Cu on the plants, which may result in a weaker ability to mobilize Fe from the roots to the aerial parts.

*Cu dynamics in soil and plants with and without magnNPs: remediation perspectives.* With the input of Cu in the soils, the amount of Cu was increased in plants (Fig. 4) and in the leaching solutions (Table 4). Remarkably, the leaching of Cu was decreased by 37% in Cu-contaminated soil enriched with magnNPs ( $1054.5 \pm 104.4 \mu\text{g}$ ) relative to magnNP-free soil ( $1618.8 \pm 81.5 \mu\text{g}$ ). In fact, IONPs display a high affinity for Cu under relevant environmental conditions;<sup>31,32</sup> therefore, magnNPs likely scavenge Cu in the soil. As a consequence, magnNPs were expected to decrease Cu bioavailability and/or assimilation by the plants, which did not occur (Fig. 4). Cu adsorbed onto magnNPs was still available for root uptake. On the other hand, because Cu adsorption onto the magnNP surface is even more favoured with increasing Cu concentrations,<sup>33</sup> lower leaching of Cu occurred in magnNP-Cu soil relative to magnNP-soil. Eventually, since plants from magnNP-Cu columns were affected by Cu toxicity, it is likely that the concentration of Cu was too high to allow magnNPs to scavenge

**Table 4** Initial Fe and Cu amounts (mg) in the soils ( $n = 4$ ) and the final Fe and Cu leaching amounts ( $\mu\text{g}$ ) measured in the released soil solutions ( $n = 4$ ) by ICP-MS after 37 days. For the ICP-MS results, different letters indicate significant differences among treatments ( $p < 0.05$ )

	Total Fe (mg) expected in 120 g soils <sup>1</sup>	Total Fe from NPs (mg) in 120 g soils <sup>a</sup>	Fe ( $\mu\text{g}$ ) in released soil solution <sup>b</sup>	$\text{Fe}^{2+}$ ( $\mu\text{g}$ ) in released soil solution <sup>c</sup>	Total Cu (mg) in 120 g soils <sup>d</sup>	Cu ( $\mu\text{g}$ ) in released soil solution
Control	3385	—	$598 \pm 78^{\text{A}}$	$339 \pm 37^{\text{A}}$	2.3	$14.4 \pm 1.0^{\text{E}}$
MagnNPs	4254	869	$2093 \pm 655^{\text{B}}$	$623 \pm 48^{\text{B}}$	2.3	$16.9 \pm 1.5^{\text{E}}$
MagnNPs-	4254	869	$549 \pm 43^{\text{C}}$	$185 \pm 8^{\text{C}}$	60	$1054.5 \pm 104.4^{\text{F}}$
Cu	3385	—	$496 \pm 16^{\text{D}}$	$269 \pm 4^{\text{D}}$	60	$1618.8 \pm 81.5^{\text{G}}$

<sup>a</sup> Theoretical calculations based on the molar mass of Fe and O (and the initial Fe(II)/Fe(III) ratio of magnNPs). <sup>b</sup> Fe ( $\mu\text{g}$ ) amount (ionic and colloidal forms) calculated from ICP-MS measurements. <sup>c</sup>  $\text{Fe}^{2+}$  ( $\mu\text{g}$ ) amount (truly dissolved) calculated from spectroscopic measurements (1,10-phenanthroline method).<sup>32</sup> <sup>d</sup> Theoretical calculation of the initial Cu in the soil (based on the Institut en Santé Agro-Environnement (Combourg, France) analyses and Cu molar mass) and addition of  $\text{CuSO}_4$ .



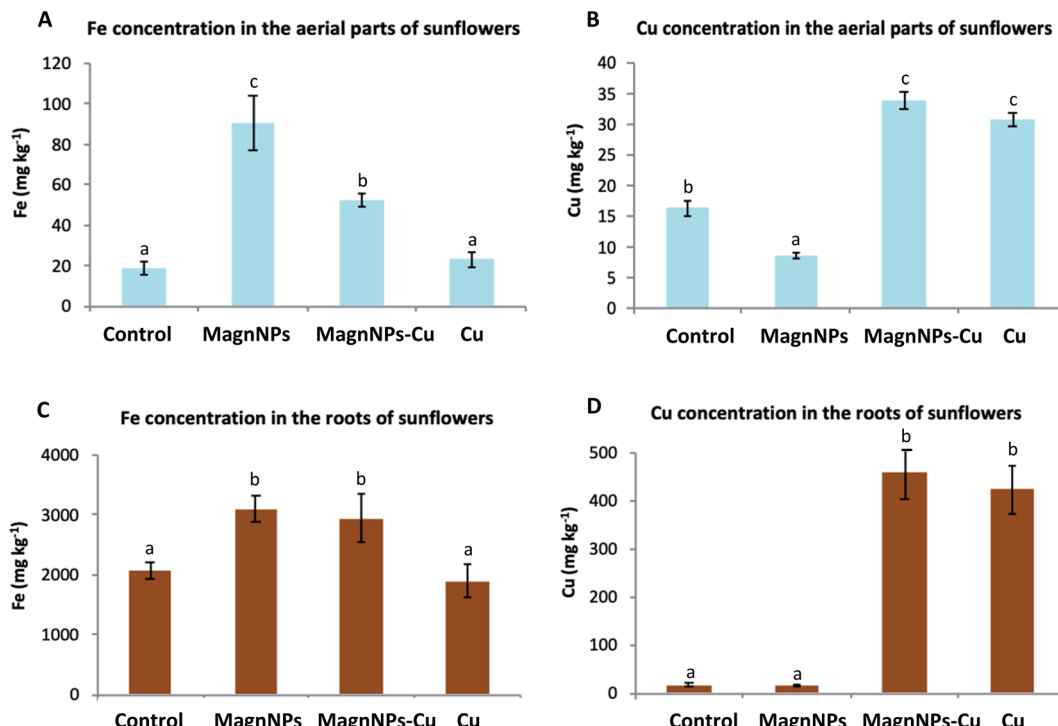


Fig. 4 Iron (Fe) and copper (Cu) concentrations ( $\text{mg kg}^{-1}$ ) in the plant tissues (aerial parts, roots) of sunflowers from the soil column experiment measured by ICP-MS after 95 days: (A) Fe concentration in the aerial parts of sunflowers, (B) Cu concentration in the aerial parts of sunflowers, (C) Fe concentration in the roots of sunflowers, (D) Cu concentration in the roots of sunflowers. Data represent the mean  $\pm$  SEM ( $n = 4$ ). Different letters above the bars indicate significant differences ( $p < 0.05$ ).

enough Cu to prevent any excess Cu in the plant tissues and subsequent Cu toxicity.

## 4. Conclusions

In conclusion, even at the high concentrations used in water/soil remediation, magnNPs are expected to have only a slight impact on the physiological and biochemical responses of sunflowers while enhancing the plant protection system against ROS. In contrast, the contamination of soils with Cu ( $500 \text{ mg kg}^{-1}$ ) considerably reduced plant growth, decreased pigment contents and induced oxidative damage to sunflowers. The occurrence of magnNPs in Cu-polluted soils did not prevent other damaging effects induced by excess Cu, despite the positive effects suggested by a decrease in lipid peroxidation. Besides, since the concentration of Cu was comparable in magnNP-Cu and Cu-exposed plants (without magnNPs), it was inferred that magnNPs did not decrease Cu bioavailability and assimilation by sunflowers. A significant increase in Fe in the tissues of plants exposed to magnNPs was observed relative to control plants, while Fe solubilization and assimilation by the plants were reduced in magnNP-Cu- and Cu-polluted soils. A decrease in magnNP uptake in magnNP-Cu plants was also evidenced by magnetic susceptibility measurements. The impacts of Cu on plant physiology and the associated biotic processes in the soil likely affected the magnNP uptake capacity of the plants as well as the regulation of Fe uptake and assimilation. Although magnNPs were not efficient in preventing the

phytotoxic effect of high Cu concentrations in soils, magnNPs were able to scavenge Cu and decrease Cu mobility in the soil without hampering Cu bioavailability. These last properties are promising assets for remediation purposes.

## Conflicts of interest

There are no conflicts to declare.

## Acknowledgements

We are thankful to the University of Rennes 1 for enabling the PhD thesis to be conducted. The study was funded by the University Rennes 1 through the 'Défis Scientifiques Emergents' program awarded to Dr Aline Dia, and the CNRS EC2CO and the Mission for Cross-cutting and Interdisciplinary Initiatives programs through 'SURFNANO' and 'ALIEN' projects, respectively, both awarded to Dr Mathieu Pédrot. We also thank the Author Services of Springer Nature for post-editing the English style. The authors are grateful to V. Dorcet for the assistance in TEM experiments performed on THEMIS platform (ScanMAT, UMS 2011 University of Rennes 1-CNRS; CPER-FEDER 2007–2014)

## References

- Y. Wang and B. Nowack, Dynamic probabilistic material flow analysis of nano- $\text{SiO}_2$ , nano iron oxides, nano- $\text{CeO}_2$ , nano-



Al<sub>2</sub>O<sub>3</sub>, and quantum dots in seven European regions, *Environ. Pollut.*, 2018, **235**, 589–601.

2 L. Wang, J. Li, Q. Jiang and L. Zhao, Water-soluble Fe<sub>3</sub>O<sub>4</sub> nanoparticles with high solubility for removal of heavy-metal ions from waste water, *Dalton Trans.*, 2012, **41**, 4544–4551.

3 R. Podila and J. M. Brown, Toxicity of engineered nanomaterials: a physico-chemical perspective, *J. Biochem. Mol. Toxicol.*, 2013, **27**(1), 50–55.

4 W. H. Suh, K. Suslick, G. D. Stucky and Y.-H. Suh, Nanotechnology, nanotoxicology, and neuroscience, *Prog. Neurobiol.*, 2009, **87**, 133–170.

5 L. R. Khot, S. Sankaran, J. M. Maja, R. Ehsani and E. W. Schuster, Applications of nanomaterials in agricultural production and crop protection: a review, *Crop Prot.*, 2012, **35**, 64–70.

6 M. Kah, S. Beulke, K. Tiede and T. Hofmann, Nanopesticides: state of knowledge, environmental fate, and exposure modeling, *Crit. Rev. Environ. Sci. Technol.*, 2013, **43**(16), 1823–1867.

7 P. Solanki, A. Bhargava, H. Chhipa, N. Jain and J. Panwar, in *Nanotechnologies in Food and Agriculture*, ed. M. Rai, C. Ribeiro, L. Mattoso and N. Duran, Springer International, 2015, ch. 4, pp. 81–101.

8 G. Batley, J. K. Kirby and M. J. McLaughlin, Fate and Risks of nanomaterials in aquatic and terrestrial environments, *Acc. Chem. Res.*, 2013, **46**(3), 854–862.

9 M. A. Ahmed, S. M. Ali, S. I. El-Dek and A. Galal, Magnetite-hematite nanoparticles prepared by green methods for heavy metal ions removal from water, *J. Mater. Sci. Eng. B*, 2013, **178**, 744–751.

10 P. N. Dave and L. V. Chopda, Application of iron oxide nanoparticles for the removal of heavy metals, *J. Nanotechnol.*, 2014, **2014**, 398569.

11 L. Goswami, K.-H. Kim, A. Deep, P. Das, S. S. Bhattacharya, S. Kumar and A. A. Adelodun, Engineered nanoparticles: nature, behavior and effects on the environment, *J. Environ. Manage.*, 2017, **196**, 297–315.

12 E. Navarro, A. Baun, R. Behra, N. B. Hartman, J. Filser, A.-J. Miao, A. Qigg, P. H. Santschi and L. Sigg, Environmental behavior and ecotoxicity of engineered nanoparticles to algae, plants and fungi, *Ecotoxicology*, 2008, **17**, 372–386.

13 V. K. Sharma, J. Filip, J. Zboril and R. S. Varma, Natural inorganic nanoparticles – formation, fate and toxicity in the environment, *Chem. Soc. Rev.*, 2015, **44**(23), 8410–8423.

14 J. Lv, P. Christie and S. Zhang, Uptake, translocation, and transformation of metal-based nanoparticles in plants: recent advances and methodological challenges, *Environ. Sci.: Nano*, 2019, **6**, 41–59.

15 T. Hiemstra and W. H. Van Riemsdijk, On the relationship between charge distribution, surface hydration and the structure of the interface of metal hydroxides, *J. Colloid Interface Sci.*, 2006, **301**(1), 1–18.

16 S. H. Joo and D. Zhao, Environmental dynamics of metal oxide nanoparticles in heterogeneous systems: a review, *J. Hazard. Mater.*, 2017, **322**, 29–47.

17 G. R. Aiken, H. Hsu-Kim and J. N. Ryan, Influence of dissolved organic matter on the environmental fate of metals, nanoparticles and colloids, *Environ. Sci. Technol.*, 2011, **45**, 3196–3201.

18 H. Zhu, J. Han, J. Q. Xiao and Y. Jin, Uptake, translocation, and accumulation of manufactured iron oxide nanoparticles by pumpkin plants, *J. Environ. Monit.*, 2008, **10**, 713–717.

19 J. Li, P. R. Chang, J. Huang, Y. Wang, H. Yuan and H. Ren, Physiological effects of magnetic iron oxide nanoparticles towards watermelon, *J. Nanosci. Nanotechnol.*, 2013, **13**, 5516–5567.

20 J. Li, J. Hu, C. Ma, Y. Wang, C. Wu, J. Huang and B. Xing, Uptake, translocation and physiological effects of magnetic iron oxide ( $\gamma$ -Fe<sub>3</sub>O<sub>4</sub>) nanoparticles in corn (*Zea mays* L.), *Chemosphere*, 2016, **159**, 326–334.

21 D. K. Tripathi, Shweta, S. Singh, S. Singh, R. Pandey, V. P. Singh, N. C. Sharma, S. M. Prasad, N. K. Dubey and D. K. Chauhan, An overview on manufactured nanoparticles in plants: uptake, translocation, accumulation and phytotoxicity, *Plant Physiol. Biochem.*, 2017, **110**, 2–12.

22 R. Barrena, E. Casals, J. Colon, X. Font, A. Sanchez and V. Puntes, Evaluation of the ecotoxicity of model nanoparticles, *Chemosphere*, 2009, **75**, 850–857.

23 F. Perreault, M. Samadani and D. Dewez, Effect of soluble copper released from copper oxide nanoparticles solubilization on growth and photosynthetic processes of *Lemnagibba* L., *Nanotoxicology*, 2013, **8**(4), 374–382.

24 A. Rastogi, M. Zivcak, O. Sytar, H. M. Kalaji, X. He, S. Mbarki and M. Breistic, Impact of metal and metal oxide nanoparticles on plant: a critical review, *Front. Chem.*, 2017, **5**, 78–94.

25 M. Tatari, R. F. Ghazvini, N. Etemadi, A. M. Ahadi and A. Mousavi, Analysis of Antioxidant Enzymes Activity, Lipid Peroxidation and Proline Content of *Agropyron desertorum* Under Drought Stress, *South Western Journal of Horticulture, Biology and Environment*, 2012, **3**(1), 9–24.

26 C. Huth, L. M. Mertz-Henning, S. J. Lopes, L. A. Tabaldi, L. V. Rossato, F. C. Krzyzanowski and F. A. Henning, Susceptibility to weathering damage and oxidative stress on soybean seeds with different lignin contents in the seed coat, *J. Seed Sci.*, 2016, **38**(4), 296–304.

27 M. Adrees, S. Ali, A. Rizwan, M. Ibrahim, F. Abbas, M. Farid, M. Zia-ur-Rehman, M. Kashif Irshad and S. Aslam Bharwana, The effect of excess copper on growth and physiology of important food crops: a review, *Environ. Sci. Pollut. Res.*, 2015, **22**, 8148–8162.

28 A. Michaud, M. Bravin, M. Galleguillos and P. Hinsinger, Copper uptake and phytotoxicity as assessed in situ for durum wheat (*Triticum turgidum*, durum L.) cultivated in Cu-contaminated, former vineyard soils, *Plant Soil*, 2007, **298**(1–2), 99–111.

29 E. Besnard, C. Chenu and M. Robert, Influence of organic amendments on copper distribution among particle-size and density fractions in Champagne vineyard soils.



*Environmental Pollution*, 9 (2001). Copper in plants, *Braz. J. Plant Physiol.*, 2005, **17**(1), 145–156.

30 K. A. Mackie, T. Müller and E. Kandeler, Remediation of copper in vineyards – a mini review, *Environ. Pollut.*, 2012, **167**, 16–26.

31 I. Yruela, Copper in Plants, *Braz. J. Plant Physiol.*, 2005, **17**(1), 145–156.

32 J.-F. Liu, Z.-S. Zhao and G.-B. Jiang, Coating  $\text{Fe}_3\text{O}_4$  Magnetic Nanoparticles with Humic Acid for High efficient Removal of Heavy Metals in water, *Environ. Sci. Technol.*, 2008, **42**, 6949–6954.

33 E. Demangeat, M. Pédrot, A. Dia, M. Bouhnik-Le-Coz, M. Davranche and F. Cabello-Hurtado, Surface modifications at the oxide/water interface: implications for Cu binding, solution chemistry and stability of iron oxide nanoparticles, *Environ. Pollut.*, 2020, **257**, 113626.

34 B. Rutkowska, W. Szulc and K. Bomze, Effects of soil properties on copper speciation in soil solution, *J. Elem.*, 2013, **18**, 695–703.

35 E. Demangeat, M. Pédrot, A. Dia, M. Bouhnik-Le-Coz, F. Grasset, K. Hanna, M. Kamagata and F. Cabello-Hurtado, Colloidal and chemical stabilities of iron oxide nanoparticles in aqueous solutions: the interplay of structural, chemical and environmental drivers, *Environ. Sci.: Nano*, 2018, **5**, 992–1001.

36 M. Komárek, A. Vaněk and V. Ettler, Chemical stabilization of metals and arsenic in contaminated soils using oxides – a review, *Environ. Pollut.*, 2013, **172**, 9–22.

37 J. Lin, W. Jiang and D. Liu, Accumulation of copper by roots, hypocotyls, cotyledons and leaves of sunflower (*Helianthus annuus* L.), *Bioresour. Technol.*, 2003, **86**, 151–155.

38 P. Soudek, S. Petrova, D. Benesova and T. Vanek, Phytoextraction of toxic metals by sunflower and corn plants, *J. Food, Agric. Environ.*, 2010, **8**(3 and 4), 383–390.

39 D. R. Hoagland and D. I. Arnon, The water-culture method for growing plants without soil, *Circ. - Calif. Agric. Exp. Stn.*, 1950, **347**, 1–31.

40 H. K. Lichtenthaler and A. R. Wellburn, Determination of total carotenoids and chlorophyll *a* and *b* of leaf extract in different solvents, *Biochem. Soc. Trans.*, 1983, **11**, 591–592.

41 K. Rohacek and M. Bartak, Technique of the modulated chlorophyll fluorescence: basic concepts, useful parameters, and some applications, *Photosynthetica*, 1999, **37**, 339–363.

42 D. M. Hodges, J. M. DeLong, C. F. Forney and R. K. Prange, Improving the thiobarbituric acid-reactive-substances assay for estimating lipid peroxidation in plant tissues containing anthocyanin and other interfering compounds, *Planta*, 1999, **207**, 604–611.

43 M. Bradford, A rapid and sensitive method for the quantitation of microgram quantities of protein utilizing the principle of protein-dye binding, *Anal. Biochem.*, 1976, **72**, 248–254.

44 J. Putter, in *Methods of Enzymatic Analysis*, ed. H. U. Bergmeyer, Verlag Chemie, Weinheim, 2nd edn, 1974, vol. 2, pp. 685–690.

45 I. Cakmak and H. Marschner, Magnesium deficiency and high light intensity enhance activities of super oxide dismutase, ascorbate peroxidase and glutathione reductase in bean leaves, *Plant Physiol.*, 1992, **98**, 1222–1227.

46 C. N. Giannopolis and S. K. Ries, Superoxide Dismutases: I. Occurrence in higher plants, *Plant Physiol.*, 1977, **59**(2), 309–314.

47 D. Yéghicheyan, C. Bossy, M. Bouhnik Le Coz, C. Douchet, G. Granier, A. Heimburger, F. Lacan, A. Lanzanova, T. C. C. Rousseau, J. L. Seidel, M. Tharaud, F. Candaudap, J. Chmeleff, C. Cloquet, S. Delpoux, M. Labatut, R. Losno, C. Pradoux, Y. Sivry and J. E. Sonke, A compilation of silicon, rare earth element and twenty-one other trace element concentrations in the natural river water reference material slrs-5 (nrc-cnrc), *Geostand. Geoanal. Res.*, 2013, **37**(4), 449.

48 D. P. Maxbauer, J. M. Feinberg, D. L. Fox and E. A. Nater, Response of pedogenic magnetite to changing vegetation in soils developed under uniform climate, topography, and parent material, *Sci. Rep.*, 2017, **7**, 17575–17785.

49 J. Lin, W. Jiang and D. Liu, Accumulation of copper by roots, hypocotyls cotyledons and leaves of sunflower (*Helianthus annuus* L.), *Bioresour. Technol.*, 2003, **86**, 151–155.

50 R. Manivasagaperumal, P. Vijayarengengan, S. Balamurugan and G. Thiyagarajan, Effect of copper on growth, dry matter yield and nutrient content of *Vigna Radiata* (L.), *Wilczek. J. Phytol.*, 2011, **3**(3), 53–62.

51 R. Esteban, O. Barruia, U. Artetxe, B. Fernandez-Marin, A. Hernandez and J. I. Garcia-Plazaola, Internal and external factors affecting photosynthetic pigment composition in plants: a meta-analytical approach, *New Phytol.*, 2015, **206**, 268–280.

52 P. K. Yudina, L. A. Ivanova, D. A. Rhondina, N. V. Zolotareva and L. A. Ivanov, Variation of leaf traits and pigment content in three species of steppe plants depending on climate aridity, *Russ. J. Plant Physiol.*, 2017, **64**(3), 410–422.

53 H. Qian, X. Peng, X. Han, J. Ren, L. Sun and Z. Fu, Comparison of the toxicity of silver nanoparticles and silver ions on the growth of terrestrial plant model *Arabidopsis thaliana*, *J. Environ. Sci.*, 2013, **25**, 1947–1956.

54 S. Dey, P. B. Mazumder and S. B. Paul, Effect of copper on growth and chlorophyll content in tea plants (*Camellia sinensis* (L.) O. Kuntze), *International Journal of Research in Applied, Natural and Social Sciences*, 2014, **2**(5), 223–230.

55 G. Ouzounidou, Copper induced changes on growth, metal content and photosynthetic function of *Alyssum montanum* L. plants, *Environ. Exp. Bot.*, 1994, **34**(2), 165–172.

56 T. Baszynsk, A. Tukendorf, M. Ruszkowska, E. Skorzynska and W. Maksymiec, Characteristics of the photosynthetic apparatus of copper non tolerant spinach exposed to excess copper, *J. Plant Physiol.*, 1988, **132**, 708–713.

57 Z. Siddique, K. P. Akhtar, A. Hameed, N. Sarwar, I. U. Haq and S. A. Khan, Biochemical alterations in leaves of resistant and susceptible cotton genotypes infected systemically by cotton leaf curl Burewala virus, *J. Plant Interact.*, 2014, **9**(1), 702–711.



58 M. F. Iannone, M. D. Groppe, M. E. de Sousa, M. Beatriz Fernandez van Raapand and M. P. Benavides, Impact of Magnetite Iron Oxide nanoparticles on wheat (*Triticum aestivum L.*) development: evaluation of oxidative damage, *Environ. Exp. Bot.*, 2016, **131**, 77–88.

59 M. G. M. Palmqvist, G. A. Seisenbaeva, P. Svedlindh and V. G. Kessler, Maghemite Nanoparticles Act as Nanoenzymes, Improving Growth and Abiotic Stress Tolerance in *Brassica napus*, *Nanoscale Res. Lett.*, 2017, **12**, 631–640.

60 A. Praveen, E. Khan, S. Ngiimei D, M. Pervez, M. Sadar and M. Gupta, Iron Oxide Nanoparticles as Nano-adsorbents: A Possible Way to Reduce Arsenic Phytotoxicity in Indian Mustard Plant (*Brassica juncea L.*), *J. Plant Growth Regul.*, 2018, **37**(2), 612–624.

61 T. Abedi and H. Pakniyat, Antioxidant Enzyme Changes in Response to Drought Stress in Ten Cultivars of Oilseed Rape (*Brassica napus L.*), *Czech J. Genet. Plant Breed.*, 2010, **46**(1), 27–34.

62 R. G. Alscher, N. Erturk and L. S. Heath, Role of superoxide dismutases (SODs) in controlling oxidative stress, *J. Exp. Bot.*, 2002, **5**, 1331–1341.

63 S. Gao, C. Ouyang, S. Wang, Y. Xu, L. Tang and F. Chen, Effects of salt stress on growth, antioxidant enzyme and phenylalanine ammonia-liase activities in *Jatropha curcas L.* seedlings, *Plant, Soil Environ.*, 2008, **54**(9), 374–381.

64 J. Patykowski and J. Kolodziejek, Changes in Antioxidant Enzyme Activities of European Mistletoe (*Viscum album L.* subsp. *Album*) Leaves as a Response to Environmental Stress Caused by Pollution of the Atmosphere by Nitrogen Dioxide, *Pol. J. Environ. Stud.*, 2016, **25**(2), 725–732.

65 N. Liu, Z. Lin, L. Guan, G. Gaughan and G. Lin, Antioxidant Enzymes Regulate Reactive Oxygen Species during Pod Elongation in *Pisum sativum* and *Brassica chinensis*, *PLoS One*, 2014, **9**(2), 1–9.

66 E. Birben, U. M. Sahiner, C. Sackesen, S. Erzurum and O. Kalayci, Oxidative Stress and Antioxidant Defense, *World Allergy Organ. J.*, 2012, **5**(1), 9–19.

67 W. Wu, X. Wan, F. Shah, S. Fahad and J. Huang, The Role of Antioxidant Enzymes in Adaptive Responses to Sheath Blight Infestation under Different Fertilization Rates and Hill Densities, *Sci. World J.*, 2014, **2014**, 502134.

68 N. A. Anjum, M. A. Merios Rodrigo, A. Moulick, Z. Heger, P. Kopel, O. Zitka, V. Adam, A. S. Lukatkin, A. C. Duarte, E. Pereira and R. Kizek, Transport phenomena of nanoparticles in plants and animals/humans, *Environ. Res.*, 2016, **151**, 233–243.

69 M. Amde, J.-F. Liu, Z.-Q. Tan and D. Bekana, Transformation and bioavailability of metal oxide nanoparticles in aquatic and terrestrial environments. A review, *Environ. Pollut.*, 2017, **230**, 250–267.

70 P. Miralles, T. L. Church and A. T. Harris, Toxicity, Uptake, and Translocation of Engineered Nanomaterials in Vascular plants, *Environ. Sci. Technol.*, 2012, **46**, 9224–9239.

71 H. Lequeux, C. Hermans, S. Lutts and N. Verbruggen, Response to copper excess in *Arabidopsis thaliana*: impact on the root system architecture, hormone distribution, lignine accumulation and mineral profile, *Plant Physiol. Biochem.*, 2010, **48**, 673–682.

72 Z. Cifuentes, L. Custardoy, J. M. de la fuente, C. Marquina, M. R. Ibarra, D. Rubiales and A. Peres-de-Luque, Absorption and translocation to the aerial part of magnetic carbon-coated nanoparticles through the root of different crop plants, *J. Nanobiotechnol.*, 2010, **8**, 8–26.

73 M. Al-Sid-Cheikh, M. Pédrot, A. Dia, M. Davranche, L. Jeanneau, P. Petitjean, M. Bouhnik-Le Coz, M.-A. Cormier and F. Grasset, Trace element and organic matter mobility impacted by  $Fe_3O_4$ -nanoparticle surface coating within wetland soil, *Environ. Sci.: Nano*, 2019, **6**, 3049–3059.

74 B. K. G. Theng and G. Yuan, Nanoparticles in the soil environment, *Elements*, 2008, **4**, 395–399.

75 F. Reith and G. Cornelis, Effect of soil properties on gold- and platinum nanoparticle mobility, *Chem. Geol.*, 2017, **466**, 446–453.

76 O. Sagee, I. H. Dror and B. Berkowitz, Transport of silver nanoparticles (AgNPs) in soil, *Chemosphere*, 2012, **88**, 670–675.

77 S. Bastani, R. Hajiboland, M. Khatamian and M. Saket-Oskoui, Nano iron (Fe) is an effective source of Fe for Tobacco plants grown under low Fe supply, *J. Soil Sci. Plant Nutr.*, 2018, **18**(2), 524–541.

78 J. Yuan, Y. Chen, H. Li, J. Lu, H. Zhao, M. Liu, G. S. Nechitaylo and N. N. Guschchenko, New insights into the cellular responses to iron nanoparticles in *Capsicum annuum*, *Sci. Rep.*, 2018, **8**(1), 3228.

79 K. M. Keiblunger, M. Schneider, M. Gorfer, M. Paumann, E. Deltedesco, H. Berger, L. Jöchlunger, A. Mentler, S. Zechmeister-Boltenstern, G. Soja and F. Zehetner, Assessment of Cu application in two contrasting soils-effects on soil microbial activity and the fungal activity structure, *Ecotoxicology*, 2018, **27**, 217–233.

80 P. Karimi, R. A. Khavari-Nejad, V. Niknam, F. Ghahremaninejad and F. Najafi, The effects of excess copper on antioxydative enzymes, lipid peroxidation, proline, chlorophyll, and concentration of Mn, Fe and Cu in *Astragalus neo-mobayenii*, *Sci. World J.*, 2012, **2012**, 615670.

